Generalized dimer states

1994 J. Phys.: Condens. Matter 6 2773

(http://iopscience.iop.org/0953-8984/6/14/015)

J. Phys.: Condens. Matter 6 (1994) 2773–2786. Printed in the UK

Generalized dimer states

M W Long and C A Hayward
School Of Physics, Birmingham University, Edgbaston, Birmingham B15 2TT, UK

Received 17 January 1994

Abstract. We present a new class of variational wavefunctions that can be used to investigate quantum antiferromagnetic systems. The states are a natural generalization of the nearest-neighbour dimer phases which have been thoroughly studied in the literature. We describe a one-dimensional class of total-spin-singlet wavefunctions, which include as special cases the two nearest-neighbour dimer phases and the exact solution to the total-spin-two projector Hamiltonian. These different solutions are 'smoothly' interpolated by a range of singlets with short-range correlations. Although the states have only short-range order, we can obtain over 98% of the ground-state energy of the nearest-neighbour Heisenberg model. We apply our basis to the J_1–J_2 Heisenberg model and the single hole in the t_1–t_2 infinite-U Hubbard model, successfully predicting the behaviour observed in finite-size scaling calculations.

1. Introduction

Classical magnetism is concerned primarily with ordered states. Quantum corrections introduce 'fluctuations' that tend to reduce the degree of order, but usually quantum mechanics can safely be ignored as a 'renormalization' of parameters. In rare situations, however, quantum mechanics can fundamentally change the physics of a quantum magnet: in one dimension, long-range order is destroyed by quantum mechanical fluctuations (if there are any), and an interesting state with a power-law decay of correlations and 'self-similar' characteristics replaces it [1]. For heavily frustrated systems in any dimension, so-called 'dimer' phases with only short-range spin correlations and a gap to excitations can also be stabilized [2]. In this paper we will look at possible ways to describe dimer states in spin-half systems, developing some bases which can be used to perform variational calculations on most types of dimer state. We are not the first to use this type of construction [3], although our particular approach appears to be new.

Although the basic idea can be used to provide a *complete* basis if required, we will dominantly be concerned with applications that involve only exponential decay of correlation functions. We will *not* therefore be describing gapless systems involving a power-law decay of correlation functions, but only dimer phases. We will devote some thought to the gapless phases, however, showing that there are fairly long-range remnants of any divergence in our calculations, a signature that would be difficult to miss.

It has proven possible to evaluate some correlation functions in our description and we will provide examples of spin–spin correlation functions and also ring-exchange or cyclic-permutation correlations, which are important in a proper description of the one-dimensional Heisenberg model and phase transitions between gapless and gapped states (see the appendix).

We have selected two physical examples for use as applications of our ideas. First, the J_1–J_2 Heisenberg model, with nearest-neighbour and next-nearest-neighbour interactions,

0953-8984/94/142773+14$19.50

which exhibits a phase transition between a gapless and gapped phase. Second, a single hole in the t_1–t_2 infinite-U Hubbard model, with competing nearest-neighbour and next-nearest-neighbour hopping, which has surprisingly rich behaviour with the spin density shifting around dramatically in reciprocal space.

In section 2 we describe the mathematical ideas behind the calculations, in section 3 we perform the correlation function calculations, in section 4 we look at the J_1–J_2 Heisenberg model, in section 5 we analyse a single hole in the t_1–t_2 infinite-U Hubbard model, and in section 6 we present our conclusions.

2. The basis of total-spin-singlet states

The fundamental physical idea that we make use of is that a *complete* basis of total-spin-singlet states for a spin-half system can be obtained using non-interleaved singlets running between two sublattices [4]. This description requires an ordering, and then the two sublattices alternate along this ordering. A total-spin-singlet state is created by laying down singlets with one end on one sublattice and the other end on the other sublattice. The basis composed of all such states is overcomplete and we require a restriction in order to form a linearly independent basis. One choice of restriction is that to *non-interleaved* states: a non-interleaved state is one for which, when any two singlets are considered, both ends of one singlet are always between the ends of the other. States with this restriction form a complete linearly independent but non-orthogonal basis [4].

This choice of representation yields a new description for the total-spin-singlet subspace, but its success will be controlled by its ease of use and predictive power. In this paper we propose simple methods of using this representation, or at least sizable subsets of it, to perform analytical calculations on simple one-dimensional models.

Our first task is to obtain a formal way to represent our chosen states, and for this we have elected to use a nearest-neighbour dimer state, combined with transposition operators. We choose (arbitrarily) one of the two nearest-neighbour dimer states and use a label, j say, to label either the singlets or one of the sublattices along the ordering. We then consider the transposition operators, $\hat{P}_j$ say, which transpose the two neighbouring spins on the jth singlet and the $(j+1)$th singlet. All these operators commute, and we can therefore create a subspace of total-spin singlets with

$$|\chi^1\chi^2.....\chi^{N-1}\rangle = \hat{P}_1^{\chi^1}\hat{P}_2^{\chi^2}.....\hat{P}_{N-1}^{\chi^{N-1}}|D\rangle \tag{2.1}$$

where N is the number of *singlets*, $|D\rangle$ is the dimer state, and the variables χ^j take the values 0 and 1. This leads to a binary description of 2^{N-1} singlet states, and we will do the majority of our analysis on this subspace. To generate the rest of the singlet space we have to resort to a 'hierarchical' construction. We next consider the transposition operators, $\hat{Q}_j$, which transpose the two neighbouring spins that compose the original jth singlet. Such an operator only yields a linearly independent state if it acts on a state for which both $\hat{P}_j$ *and* $\hat{P}_{j-1}$ are present. We therefore obtain a second 'level' of states:

$$|(\chi'^2\chi'^3.....\chi'^{N-1})(\chi^1\chi^2.....\chi^{N-1})\rangle = \hat{Q}_2^{\chi'^2}\hat{Q}_3^{\chi'^3}.....\hat{Q}_{N-1}^{\chi'^{N-1}}\hat{P}_1^{\chi^1}\hat{P}_2^{\chi^2}.....\hat{P}_{N-1}^{\chi^{N-1}}|D\rangle \tag{2.2}$$

where the value of χ'^j is zero unless *both* χ^j and χ^{j-1} are equal to one. Obviously χ'^1 is unused because there is no corresponding χ^1. The next hierarchy of states is created by applying the $\hat{P}_j$ operators to states which have both $\hat{Q}_j$ and $\hat{Q}_{j+1}$ present, and it should

be easy for the reader to see how to construct the entire singlet space hierarchically. It is straightforward to show that all non-interleaved states can be constructed in this way, and it has previously been proved that these states form a linearly independent complete basis[4].

Although this representation allows us to describe sizable numbers of total-spin singlets, there is one important drawback: the states are non-orthogonal. In order to make use of these states this problem has to be overcome. Fortunately, it is possible to control the overlap between different singlet states using the simple idea that $\langle D_1|D_2\rangle = \pm 1/2^{N_{\text{ineq}}-N_{\text{loop}}}$, where N_{ineq} is the number of inequivalent singlets in the two dimer states and N_{loop} is the number of 'closed loops' composed of pairs of singlets on both dimers. To find a closed loop, alternate between the two dimer states, hopping from one end of a singlet to the other, until you return to the initial atom. For the states encountered in the first hierarchy, each initial isolated operator $\hat{P}_j$ makes two new inequivalent singlets and one loop, and each subsequent neighbouring operator $\hat{P}_{j\pm1}$ makes one new inequivalent singlet with no new closed loops, so

$$\left\langle D\left|\prod_{j\in J}\hat{P}_j\right|D\right\rangle = \frac{1}{2^{N_J}} \tag{2.3}$$

where N_J is the number of the $\hat{P}_j$, independent of their configuration. This result enables us to orthogonalize our subspace generated by the first hierarchy, since each $\hat{P}_j$ may be treated independently.

We have elected not to work with our arbitrarily chosen dimer as the 'vacuum' for technical reasons, and instead we introduce a single-parameter family of vacua:

$$|x\rangle = \prod_j(\alpha - \beta\hat{P}_j)|D\rangle \tag{2.4a}$$

where $x = \alpha\beta$, and normalization is ensured by $\alpha^2 + \beta^2 = 1 + \alpha\beta = 1 + x$, from which it can be deduced that

$$\alpha = \tfrac{1}{2}[\sqrt{(1+3x)} + \sqrt{(1-x)}] \tag{2.4b}$$

$$\beta = \tfrac{1}{2}[\sqrt{(1+3x)} - \sqrt{(1-x)}] \tag{2.4c}$$

in terms of the single parameter x, which we choose to vary between $-1/3$ and 1.

This family of wavefunctions includes several cases which have previously been considered in the literature: the two Majumdar–Ghosh ground states [2], and the ground state to the 'P_2' projector Hamiltonian [5]. Obviously, the special value $x = 0$ corresponds to one of the nearest-neighbour dimer states, but the value $x = 1$ corresponds to the other: this value yields $\alpha = 1 = \beta$, and therefore yields a state which is *antisymmetric* under the action of all the $\hat{P}_j$, which must in turn imply that all such pairs of atoms are in total-spin singlets. The special value $x = -1/3$ yields $\alpha = 1/\sqrt{3} = -\beta$, and so leads to a state which is *symmetric* under the action of all the $\hat{P}_j$, which must in turn imply that all such pairs are in total-spin-triplet configurations. Since the original singlet remains attached by each end to its neighbouring triplets, this state must be the unique ground state to the Hamiltonian which penalizes total-spin-two configurations between neighbouring spin-one atoms. Our class of wavefunctions smoothly interpolates between these states, allowing states with a variety of short-range correlations.

Since there are two degrees of freedom per $\hat{P}_j$, namely present or not-present, we can also define an 'excitation':

$$d_j^\dagger|x\rangle \equiv \left(\prod_{j'\neq j}(\alpha - \beta\hat{P}_{j'})\right)(\gamma - \delta\hat{P}_j)|D\rangle \tag{2.5a}$$

where $\gamma^2 + \delta^2 = 1 + \gamma\delta \equiv 1 + y$. It can be shown that $x + y = \frac{2}{3}$ and therefore that

$$\gamma = \frac{1}{2}\left(\sqrt{3}\sqrt{(1-x)} - \frac{\sqrt{(1+3x)}}{\sqrt{3}}\right) \tag{2.5b}$$

$$\delta = \frac{1}{2}\left(\sqrt{3}\sqrt{(1-x)} + \frac{\sqrt{(1+3x)}}{\sqrt{3}}\right) \tag{2.5c}$$

in terms of x.

It should be clear that in this first hierarchy of states the operators $\hat{P}_j$ are treated *exactly*, yielding states that are entirely contained within the chosen subspace. Since next-nearest-neighbour exchange may be written down in the form of either $\hat{P}_j\hat{Q}_j\hat{P}_j$ or $\hat{P}_{j-1}\hat{Q}_j\hat{P}_{j-1}$, we can handle any problem involving nearest-neighbour or next-nearest-neighbour exchange, if we can represent the $\hat{Q}_j$ in our chosen subspace.

It is straightforward but tedious to show that

$$\langle x|\hat{Q}_j|x\rangle = a(x) = -\tfrac{1}{4} + \tfrac{3}{4}x^2 - \tfrac{3}{4}(1-x)\sqrt{(1-x)}\sqrt{(1+3x)} \tag{2.6a}$$

$$\langle x|\hat{Q}_j d_j^\dagger|x\rangle = \langle x|\hat{Q}_j d_{j-1}^\dagger|x\rangle = b(x) = \tfrac{\sqrt{3}}{4}[3x(1-x) + x\sqrt{(1-x)}\sqrt{(1+3x)}] \tag{2.6b}$$

$$\langle x|d_j\hat{Q}_j d_j^\dagger|x\rangle = \langle x|d_{j-1}\hat{Q}_j d_{j-1}^\dagger|x\rangle = d(x) = \tfrac{3}{4} + \tfrac{1}{2}x - \tfrac{3}{4}x^2 + \tfrac{1}{4}(1-3x)\sqrt{(1-x)}\sqrt{(1+3x)} \tag{2.6c}$$

$$\langle x|d_{j-1}\hat{Q}_j d_j^\dagger|x\rangle = \langle x|\hat{Q}_j d_j^\dagger d_{j-1}^\dagger|x\rangle = d(x) - 1 \tag{2.6d}$$

$$\begin{aligned}\langle x|d_j\hat{Q}_j d_j^\dagger d_{j-1}^\dagger|x\rangle &= \langle x|d_{j-1}\hat{Q}_j d_j^\dagger d_{j-1}^\dagger|x\rangle = f(x)\\ &= \tfrac{\sqrt{3}}{4}(x - \tfrac{2}{3})[(1+3x) + \sqrt{(1-x)}\sqrt{(1+3x)}]\end{aligned} \tag{2.6e}$$

$$\langle x|d_{j-1}d_j\hat{Q}_j d_j^\dagger d_{j-1}^\dagger|x\rangle = g(x) = -\tfrac{1}{4} + \tfrac{3}{4}(x - \tfrac{2}{3})^2 + \tfrac{1}{4}(1+3x)\sqrt{(1-x)}\sqrt{(1+3x)} \tag{2.6f}$$

where all quantities are real, from which the Hermitian conjugates can be deduced.

Using the operation of $\hat{P}_j$ on our basis

$$\hat{P}_j|x\rangle = \left(A(x) - B(x)d_j^\dagger\right)|x\rangle \tag{2.7a}$$

$$\hat{P}_j d_j^\dagger|x\rangle = \left(-B(x) - A(x)d_j^\dagger\right)|x\rangle \tag{2.7b}$$

where

$$A(x) = \tfrac{1}{2}(1-3x) \tag{2.7c}$$

$$B(x) = \tfrac{\sqrt{3}}{2}\sqrt{(1-x)}\sqrt{(1+3x)}. \tag{2.7d}$$

We are now in a position to construct any *simple* Hamiltonian in our chosen basis.

Perhaps the simplest interesting Hamiltonian is the J_1–J_2 Heisenberg Hamiltonian:

$$H = J_1 \sum_i S_i \cdot S_{i+1} + J_2 \sum_i S_i \cdot S_{i+2} \tag{2.8}$$

which becomes

$$H = \frac{J}{2} \sum_j [\hat{P}_j + \hat{Q}_j - 1 + \lambda(\hat{P}_j \hat{Q}_j \hat{P}_j + \hat{P}_{j-1} \hat{Q}_j \hat{P}_{j-1} - 1)] \tag{2.9}$$

where we have set $J_1 \equiv J$ and $J_2 = \lambda J$. In out first hierarchy space this reduces to

$$\begin{aligned} H = N a_0 &+ 2a_1 \sum_j d_j^\dagger d_j + a_2 \sum_j [d_j^\dagger d_{j+1} + d_{j+1}^\dagger d_j + d_{j+1}^\dagger d_j^\dagger + d_j d_{j+1}] \\ &+ a_3 \sum_j d_j^\dagger d_j d_{j+1}^\dagger d_{j+1} + 2a_4 \sum_j (d_j^\dagger + d_j) \\ &+ a_5 \sum_j [(d_j^\dagger + d_j) d_{j+1}^\dagger d_{j+1} + (d_{j+1}^\dagger + d_{j+1}) d_j^\dagger d_j] \end{aligned} \tag{2.10a}$$

where the coefficients satisfy

$$a_0 = a + A - 1 + \lambda(2A^2 a + 2B^2 d - 4ABb - 1) \tag{2.10b}$$

$$a_1 = d - a - A + \lambda[2A^2(d-a) + B^2(a + g - 2d) + 2AB(3b - f)] \tag{2.10c}$$

$$a_2 = d - 1 + \lambda[-2A^2(d-1) + 2B^2(d-1) + 2AB(f - b)] \tag{2.10d}$$

$$a_3 = a + g - 2d + \lambda[2A^2(a + g - 2d) - 2B^2(a + g - 2d) + 8AB(f - b)] \tag{2.10e}$$

$$a_4 = b - \tfrac{1}{2}B + \lambda[B^2(b + f) + AB(2 - d - a)] \tag{2.10f}$$

$$a_5 = f - b + \lambda AB(a + g + 2d - 4) \tag{2.10g}$$

where we have chosen to extract $J/2$ as our energy scale. We will look at the physics of this Hamiltonian in some detail in section 4, but there are several important conceptual points to be dealt with here.

The first key observation is that if we look at (2.10), then at face value we have a much more complicated Hamiltonian than we started with: we seem to have been going in the wrong direction! Perhaps even worse is the fact that this Hamiltonian does not conserve number locally at both the two- and *single*-particle level. Although both of these observations are true, there are some important facts which reduce their significance. Probably the most important point is that our vacuum $|x\rangle$ is a much better starting point for dimer calculations than the totally ferromagnetic state, which would otherwise be selected. We have already found the best short-range correlations in selecting x and then the $d_j^\dagger$ degrees of freedom yield only minor corrections, inducing weak additional local correlations. Also, the choice of x is intimately related to the fact that the Hamiltonian does not conserve single particles. Optimizing the energy in the absence of $d^\dagger$s is *equivalent* to choosing x so that $a_4 = 0$ and the vacuum is stable against single-particle fluctuations. Our technical decision to include the parameter x in our description is equivalent to ensuring single-particle number conservation. The natural residual role of the $d_j^\dagger$ degrees of freedom is therefore to weak pairing fluctuations, as we shall see in section 4.

The most important degree of freedom in our modelling is x, which gives the system the freedom to choose between a variety of short-range correlations. In our second application, to a single hole in the infinite-U Hubbard model with nearest- and next-nearest-neighbour hopping, the t_1–t_2 model, this degree of freedom is once again crucial. The original model is

$$H = -t_1 \sum_{i\sigma}[(1 - c^\dagger_{i\bar{\sigma}} c_{i\bar{\sigma}}) c^\dagger_{i\sigma} c_{i+1\sigma} (1 - c^\dagger_{i+1\bar{\sigma}} c_{i+1\bar{\sigma}}) + \text{CC}]$$
$$- t_2 \sum_{i\sigma}[(1 - c^\dagger_{i\bar{\sigma}} c_{i\bar{\sigma}}) c^\dagger_{i\sigma} c_{i+2\sigma} (1 - c^\dagger_{i+2\bar{\sigma}} c_{i+2\bar{\sigma}}) + \text{CC}] \tag{2.11}$$

where $c^\dagger_{i\sigma}$ creates an electron of spin σ on site i, and the restriction to single occupancy is enforced by the projection operators in brackets. Since we are dealing with a single hole, we can use Bloch's theorem to eliminate the position of the hole and use a spin-only representation for the model. We consider two states, $|x, 0\rangle$ and $|x, 1\rangle$, where the first finds the hole centred between a pair of spins transposed by $\hat{Q}_0$ and the second is a translation of the first through one atomic spacing, yielding a state with the hole centred between a pair of spins transposed by $\hat{P}_0$. We label the operators away from the hole with $\hat{P}_j$ to the right and $\hat{P}_{\bar{j}}$ to the left. Note that this choice is *not* symmetric, since there is no $\hat{P}_0$ for $|x, 0\rangle$ and no $\hat{Q}_0$ for $|x, 1\rangle$. For this choice the Hamiltonian is

$$H_0 = t[T + T^{-1} + \lambda(T^{-2}\hat{P}_{\bar{1}} + T^2 \hat{P}_{\bar{1}})] \tag{2.12a}$$

$$H_1 = t[T + T^{-1} + \lambda(T^{-2}\hat{Q}_1 + T^2 \hat{Q}_{\bar{1}})] \tag{2.12b}$$

where we have chosen to reparametrize $t_1 = t$ and $t_2 = \lambda t$, and the operator T translates through one atomic spacing. We can start with the states $|x, \chi\rangle$ and, by allowing the hole to hop progressively further away, create an increasing basis which can be described by the $d^\dagger_j$ operators. Employing the results (2.6) and (2.7) then allows us to deduce the Hamiltonian in our chosen subspace. The key step is to optimize the resulting energy over the x degree of freedom, in order to deduce the type of spin-correlations that the hole prefers to move into. We will perform these variational calculations in section 5.

3. Correlation functions

In this section we analytically solve for the spin–spin and cyclic-permutation correlation functions for our states $|x\rangle$. The fundamental reason that we can calculate these quantities is that the correlations are only short range and can therefore be controlled locally with a transfer-matrix-like technique.

We start with the easier case of the spin–spin correlations. We group the correlation functions into groups of four, considering simultaneously the correlations between the pair of spins which are transposed by $\hat{P}_0$ and the pair of spins transposed by $\hat{P}_n$. Using the commutation relations of the $\hat{P}_j$, combined with the observation that, if $\hat{O}_n \equiv \hat{P}_{1,2n}$ is the transposition that permutes the *closest* pair of the four spins, then $\hat{P}_0\hat{O}_n\hat{P}_0$, $\hat{P}_n\hat{O}_n\hat{P}_n$ and $\hat{P}_0\hat{P}_n\hat{O}_n\hat{P}_n\hat{P}_0$, constitute the other three transpositions, and all four can be written down simultaneously as

$$\langle x|\hat{P}_0^{\chi^0}\hat{P}_n^{\chi^n}\hat{O}_n\hat{P}_n^{\chi^n}\hat{P}_0^{\chi^0}|x\rangle = \langle D|\prod_{j=1}^{n-1}(1 + x - 2x\hat{P}_j)$$
$$\times (\alpha_{\chi^0} - \beta_{\chi^0}\hat{P}_0)(\alpha_{\chi^n} - \beta_{\chi^n}\hat{P}_n)\hat{O}_n(\alpha_{\chi^n} - \beta_{\chi^n}\hat{P}_n)(\alpha_{\chi^0} - \beta_{\chi^0}\hat{P}_0)|D\rangle \tag{3.1}$$

where α_χ is α if $\chi = 0$ and $-\beta$ if $\chi = 1$, and β_χ is β if $\chi = 0$ and $-\alpha$ if $\chi = 1$.

The key to evaluating this expression is to understand the action of the operators $\hat{P}_j$ in the product. Each additional $\hat{P}_j$ leads to a further inequivalent singlet with the exception of the final one. The result one obtains is therefore exactly what one would have got for the original dimer phase plus a contribution coming from the term in $\prod_{j=1}^{n-1} \hat{P}_j$. Careful consideration of this final term shows that there are two possibilities; either the final $\hat{P}_j$ makes an inequivalent singlet or it does not. For the first case there is no additional contribution, whereas for the second there is. For an even value of n an additional loop is formed, whereas for an odd value of n *two* additional loops are formed. Careful attention to detail reveals that

$$\langle x|\hat{O}_n|x\rangle = \tfrac{1}{2} - \tfrac{3}{2}(\alpha - \beta)^2\alpha^2 x^{n-1} \tag{3.2a}$$

$$\langle x|\hat{P}_0\hat{O}_n\hat{P}_0|x\rangle = \langle x|\hat{P}_n\hat{O}_n\hat{P}_n|x\rangle = \tfrac{1}{2} + \tfrac{3}{2}(\alpha - \beta)^2\alpha\beta x^{n-1} \tag{3.2b}$$

$$\langle x|\hat{P}_0\hat{P}_n\hat{O}_n\hat{P}_n\hat{P}_0|x\rangle = \tfrac{1}{2} - \tfrac{3}{2}(\alpha - \beta)^2\beta^2 x^{n-1} \tag{3.2c}$$

from which the spin–spin correlations may be immediately deduced via $\hat{P}_{1,2} = \frac{1}{2} + 2\boldsymbol{S}_1 \cdot \boldsymbol{S}_2$. The result is completed if we remember that $\boldsymbol{S}_i \cdot \boldsymbol{S}_i = \frac{3}{4}$ and that $\langle x|\hat{P}_0|x\rangle = \frac{1}{2}(1 - 3x)$.

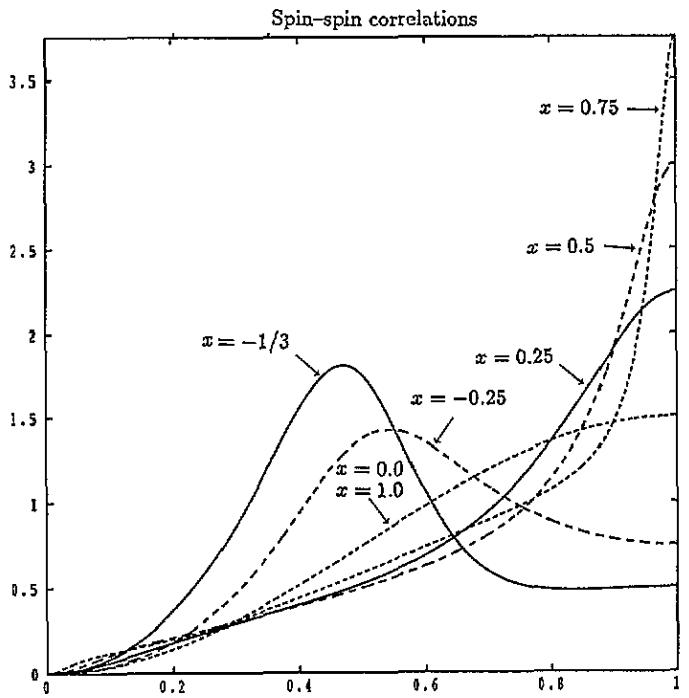

Figure 1. A sequence of calculations of the Fourier transform of the square of the spin–spin correlation functions, namely $|S_k|^2 = \sum_n \boldsymbol{S}_i \cdot \boldsymbol{S}_{i+n} \cos nak$. We have chosen to plot for values of $x = 0.75, 0.5, 0.25, 0.0, -0.25, -0.3333$; k varies from the zone centre to the zone boundary. The plots cycle through small dashes ($x = 0.75$ and 0.0), large dashes ($x = 0.5$ and -0.25), to full curves ($x = 0.25$ and $-0.333\,33$).

Transforming into reciprocal space, in order to make predictions for magnetic neutron scattering, involves summing geometric series, and we have depicted a few examples in figure 1. The exponential decay is obviously controlled by x, and when x is positive there are clearly some long-range effects present.

Our second calculation, of cyclic permutations, is less straightforward. Once again we consider four ring-exchange operators together, using the idea that if $\hat{R}_n$ pushes the spin on the atom furthest to the left to the atom furthest to the right, then $\hat{R}_n\hat{P}_0$, $\hat{P}_n\hat{R}_n$ and $\hat{P}_n\hat{R}_n\hat{P}_0$ will induce the other three cyclic permutations. All four can then be written down using

$$\left\langle x \left| \hat{R}_n(\alpha_{\chi^n} - \beta_{\chi^n}\hat{P}_n^*) \prod_{j=1,n}(\alpha - \beta\hat{Q}_j) \prod_{j=1,n}(\alpha - \beta\hat{P}_j)(\alpha_{\chi^0} - \beta_{\chi^0}\hat{P}_0) \right| x \right\rangle \quad (3.3)$$

with $\hat{P}_n^*$ being a transposition operator permuting the furthest two spins and with similar definitions to the last case for most quantities.

This expression is rather more difficult to handle, because one finds *finite* loops can be completed at different positions along the exchange. We can however 'integrate' out each atom in turn using a sort of 'transfer' matrix which counts whether or not a loop has been closed, supplying a factor two, and also including any phases from reversed singlets. For us this transfer matrix is

$$M = \begin{bmatrix} \alpha & -\beta & 0 \\ -\alpha & 0 & -\beta \\ \beta - 2\alpha & 0 & 0 \end{bmatrix} \quad (3.4)$$

in terms of which the correlation functions are

$$\frac{(-1)^n}{2^{n+1}} \begin{bmatrix} \alpha_{\chi^0} & 0 & \beta_{\chi^0} \end{bmatrix} \begin{bmatrix} \alpha & -\beta & 0 \\ -\alpha & 0 & -\beta \\ \beta - 2\alpha & 0 & 0 \end{bmatrix}^{2n} \begin{bmatrix} \alpha_{\chi^n} - 2\beta_{\chi^n} \\ -\alpha_{\chi^n} - \beta_{\chi^n} \\ \beta_{\chi^n} - 2\alpha_{\chi^n} \end{bmatrix}. \quad (3.5)$$

Once again, this result must be completed with the observation that $\langle x|\hat{R}_0|x\rangle = \frac{1}{2}(1 - 3x)$. The manner in which we start off this correlation function is subtle; for Heisenberg problems we elect to use unity as the on-site contribution. For Hubbard model problems we use negative unity for the on-site contribution, unity for the two nearest-neighbour contributions and then minus these cyclic permutations for the longer-range correlations. With this choice we are led to the change in n_k for the Hubbard model (see the appendix).

Transforming into reciprocal space is once again a collection of geometric series, with the eigenvalues of M, squared and divided by two, playing the role of the exponential decay. In figure 2 we depict a variety of the spin-model correlation functions, which we will comment on in the next section.

4. The J_1–J_2 model

Although the J_1–J_2 model is probably the simplest quantum spin model that exhibits a phase transition between a gapped and gapless phase, it has *not* been solved, and when and how the phase transition occurs can only be surmised. The point $J_2 = 0$ has been solved *via the Bethe ansatz [6], and is gapless, whereas the point* $J_1 = 2J_2$ *is trivially solved* by a dimer state [2], and is gapped. Due to the complexity of a Bethe ansatz solution, correlation functions are *not* easily calculated for the gapless model and have to be deduced

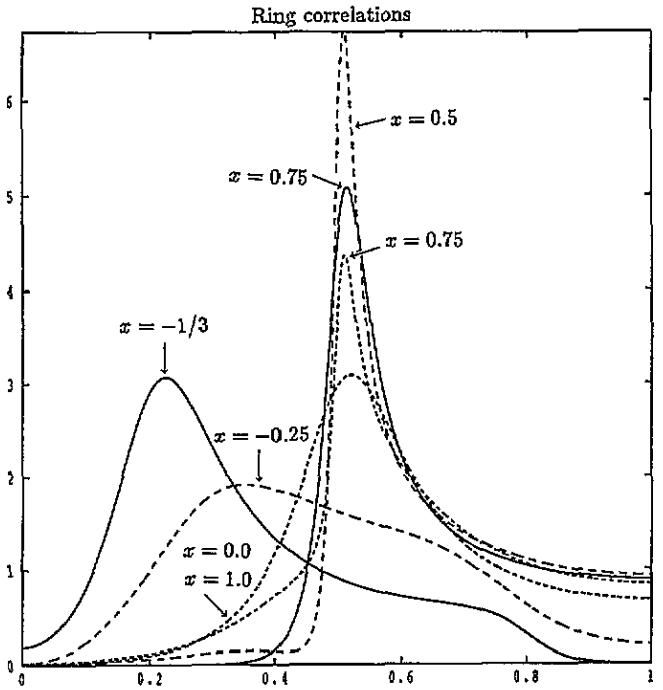

Figure 2. A sequence of calculations of the Fourier transform of the cyclic-permutation correlation functions, namely $\hat{R}_k = \sum_n \hat{R}_{i;n} \cos nak$ where $\hat{R}_{i;n}$ cyclically permutes the n-spins from the atom i, and $\hat{R}_{i;0}$ is chosen to be unity. We have chosen to plot for values of $x = 0.75, 0.5, 0.25, 0.0, -0.25, -0.3333$; k varies from the zone centre to the zone boundary. The plots cycle through small dashes ($x = 0.75$ and 0.0), large dashes ($x = 0.5$ and -0.25), to full curves ($x = 0.25$ and $-0.333\,33$).

asymptotically from the presumed continuum limit of the model [1]. On the other hand, the dimer phases are very easy to describe and any correlation function can usually be deduced almost immediately. The purpose of the current paper is to apply minor modifications to the methods which successfully yield the dimer-state correlation functions in order to try to exterpolate to the gapless phases, and to pick up any likely signature of the phase transition.

The simplest calculation one can perform is just to minimize the energy of the state $|x\rangle$ as a function of x, for each λ. As we already pointed out, this is equivalent to either minimizing a_0 or letting a_4 vanish. The behaviour of the optimum x is depicted in figure 3: for the gapless phase we have x positive, whereas for the gapped phase x drops to zero and then becomes negative. The two natural limits are $x \mapsto \frac{1}{2}$ when $J_2 \mapsto -\infty$ and $x \mapsto -\frac{1}{3}$ when $J_2 \mapsto +\infty$. The system is doing the best it can to try to emulate the different types of long-range correlations found in these limits. Energetically, the calculation is surprisingly accurate, yielding $-0.436\,83J$ for the Heisenberg ground state, less than 2% away from the exact answer $-0.443\,15J$.

The next 'natural' improvement that one can make is to apply a BCS-like theory to the second-quantized Hamiltonian of equation (2.10). We enforce only pair fluctuations, eliminating the final two terms, and then apply a mean-field argument to the remaining Hamiltonian. Obviously, since there are only two degrees of freedom per singlet, we need to use fermionic statistics for the $d_j^\dagger$ operators, but with a careful ordering of the pair operators, $d_{j+1}^\dagger d_j^\dagger$, there is no intrinsic problem. We no longer have our argument that

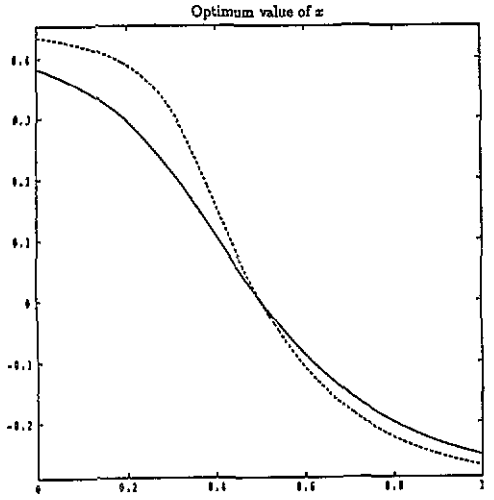

Figure 3. Calculations of the optimum value of x, calculated as a function of λ, the ratio of matrix elements in the J_1–J_2 model. The full curve employs the states $|x\rangle$, and the broken curve involves the BCS-like pairing-theory ground states.

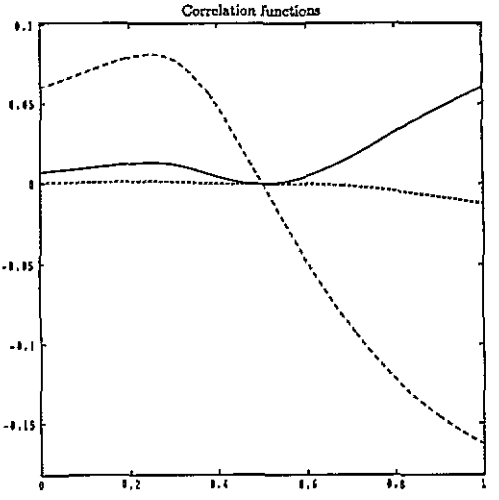

Figure 4. Plots of the three correlation functions; $\langle d_j^\dagger d_j\rangle$, $\langle d_{j+1}^\dagger d_j\rangle$ and $\langle d_{j+1}^\dagger d_j^\dagger\rangle$, as a function of the ratio of matrix elements in the J_1–J_2 Heisenberg model. The correlation functions are, respectively, the full, small-dash and large-dash broken curves.

the system does not couple to single-particle fluctuations, and we simply 'switch them off', and then optimize over x in their absence. In figure 4 we depict the single-particle correlation functions in the optimum state: $\langle d_j^\dagger d_j\rangle$, $\langle d_{j+1}^\dagger d_j\rangle$ and $\langle d_{j+1}^\dagger d_j^\dagger\rangle$. It is clear that the modifications to $|x\rangle$ are minor, although the ground-state energy for the nearest-neighbour Heisenberg model does improve to $-0.440\,01J$, less than 1% away from the exact answer. We also comment that in the region where the phase transition is expected, the number of 'excitations', namely $\langle d_j^\dagger d_j\rangle$, and the pairing correlations, namely $\langle d_{j+1}^\dagger d_j^\dagger\rangle$, both pass through a maximum. The range of the correlations is expected to increase, although we cannot prove this, being unable to evaluate the correlation functions in the presence of the $d_j^\dagger$.

Independent arguments, to do with the solitonic excitations in the system, suggest that the phase transition occurs when the cyclic-exchange correlations diverge (see the appendix). In our calculations these correlations increase with reducing J_2 without a turning point, although there is clearly an incipient instability as expected near the non-interacting 'Fermi surface', namely halfway to the zone boundary. There is no evidence from this calculation of this criterion for the phase transition.

Our calculations follow the expected behaviour of the system faithfully: the spin density moves smoothly from around the zone boundary to the 'Fermi surface' halfway to the zone boundary. There is a bifurcation of the single peak into a pair of peaks that occurs near $x \sim -0.07$, and we have some idea what to expect in broad terms. We have not learned anything fundamentally new and have not gained a lot of insight into the phase transition as yet.

5. The t_1–t_2 model

The motion of a single hole under the action of the infinite-U Hubbard model is interesting because it constitutes a new physical mechanism for lifting the spin degeneracy in a quantum

spin-half magnet. It is plausible that it is this phenomenon that occurs in perovskite superconductors, where the doping of a small concentration of holes changes the physical properties of the system dramatically.

The main difference between the spin interactions coming from hole motion and Heisenberg spin interactions, is that the hole motion is an interaction localized around the hole, whereas Heisenberg interactions are equally likely to occur anywhere in space. The energy of the hole motion is dominated by a few spins in the vicinity of the hole, but the manner in which the spin correlations spread out is energetically almost irrelevant, but physically quite interesting. The current technique yields insight into precisely this aspect of the problem.

We can use our x degree of freedom far from the hole in order to give the system a restricted but fairly wide choice of spin correlations to 'tunnel' into, and we can use our $d_j^\dagger$ degrees of freedom locally, in the vicinity of the hole, to give back the short-range correlations which are of so much importance to the energetics.

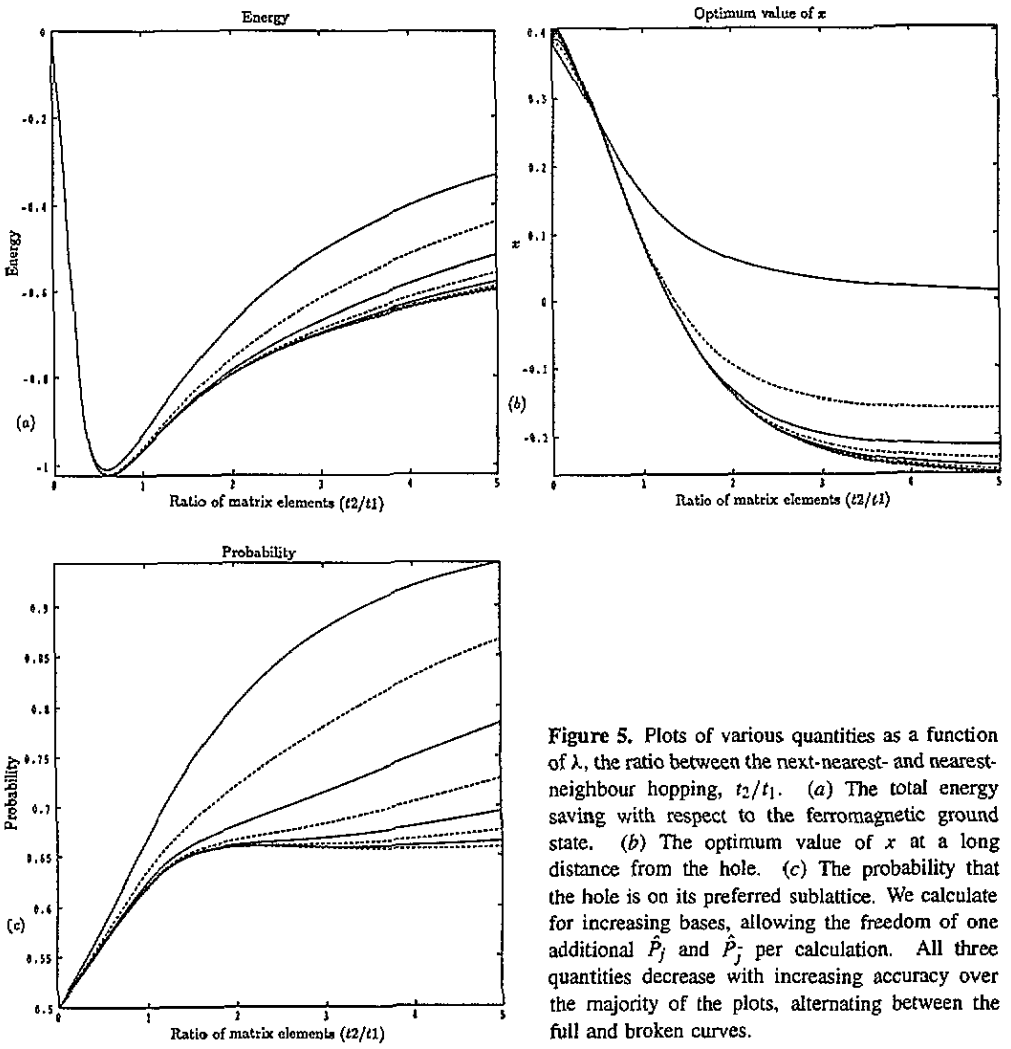

Figure 5. Plots of various quantities as a function of λ, the ratio between the next-nearest- and nearest-neighbour hopping, t_2/t_1. (*a*) The total energy saving with respect to the ferromagnetic ground state. (*b*) The optimum value of x at a long distance from the hole. (*c*) The probability that the hole is on its preferred sublattice. We calculate for increasing bases, allowing the freedom of one additional $\hat{P}_j$ and $\hat{P}_j^-$ per calculation. All three quantities decrease with increasing accuracy over the majority of the plots, alternating between the full and broken curves.

We start out with two states already described, $|x, \chi\rangle$, and then allow all possible $d_j^\dagger$

fluctuations up to a fixed finite range from the hole. We have elected to have one more degree of freedom on the $|x, 1\rangle$ state, which favours the breaking of the symmetry. We have performed a sequence of calculations allowing $2n$ mixtures of $d_j^\dagger$ for state $|x, 0\rangle$, and $2n+1$ for state $|x, 1\rangle$. We have then superimposed some plots of the physical characteristics of our solution in figure 5, for increasing values of n. The most important observation to make about the solution, is that it is *symmetry broken*: the hole selects one of the two natural sublattices as dominant and spends longer on that sublattice than on the other. Simultaneously, the spin wavefunction dimerizes, which is why our calculations are of some practical value. In figure 5(a) we plot the total energy, showing that only the larger values of $\lambda = t_2/t_1$ yield any significant effect from allowing further short-range correlations. In figure 5(b) we plot the behaviour of the optimum value of x as we change the ratio λ: we range from the closest state to the Heisenberg ground state at small λ, as analytically predicted, to close to the best that the next-nearest-neighbour Heisenberg coupling can manage as λ becomes large. In figure 5(c) we plot the probability that the hole sits on its dominant sublattice, the natural measure of the charge symmetry breaking. The easiest thing to believe is that there is no symmetry breaking in the two limits, and that the symmetry breaking is maximal near $\lambda \sim 1.5$.

This calculation is surprisingly accurate in the regime with strong symmetry breaking. For example, the 'exact' (using exact diagonalization) result for $\lambda = 2$ is $\epsilon = -4.9190t_1$, whereas our calculation predicts $\epsilon = -4.9184t_1$. The x degree of freedom at long range is more important than the short-range spin configurations omitted in our technique.

As we vary the parameter λ, the behaviour of the t_1–t_2 Hamiltonian mimics that of the J_1–J_2 Heisenberg model, with the intermediate region of dimerization found in the Heisenberg case corresponding to a symmetry-broken state for the hole where the hole chooses a preferred sublattice and the spins dimerize in order to stabilize the hole's choice.

Our calculations have proven reasonably predictive in this case, since there are no clear analytic predictions for the limit $t_1 \mapsto 0$. The only other methods of tackling this problem, namely exact diagonalization and mean-field theory, are more difficult to employ and suffer from rather different illnesses to the current calculations. Since our calculations are very simple, it is possible to make some statements about *why* the behaviour observed occurs. The fact that the optimum x drops below zero only for values of $n > 1$, indicates that the key physical process is hopping on the least preferred rail, and the corresponding introduction of longer-range loops into the most probable hopping pattern of the hole. Hopping around a *square* loop includes a cyclic exchange of three spins which contains a component of antiferromagnetic next-nearest-neighbour exchange. This simply predicts the observed behaviour, as loops of different length become more relevant.

6. Conclusions

By considering the valence-bond description of the total-spin-singlet subspace, we have developed a complete hierarchical basis for this space. If we use only the first step of the construction, then we are provided with a variational technique for analysing quantum mechanical spin problems. An even simpler restriction, to a single-parameter family of singlets, namely $|x\rangle$, appears to provide the majority of the short-range degrees of freedom, and for a problem where it is desired to find the way in which some spin degeneracy is lifted, our technique appears useful.

Although our calculations are variational, the simplicity of our wavefunctions permit us to calculate both spin–spin and cyclic-exchange correlations, and we find excellent

agreement between the short-range aspects of our solution and the exact diagonalization predictions. We are, however, completely unable to deduce anything about the power-law singularities, if present, although there are large finite peaks in our calculations which would be a clear indication of an inherent long-range phenomenon.

We have given a simple overview of the short-range behaviour of both the J_1–J_2 Heisenberg model and the single-hole t_1–t_2 infinite-U Hubbard model. The way in which the spin degeneracy is lifted is successfully predicted in both cases.

It seems clear that there are a large number of improvements that can be made to the theory, although it is not so clear whether or not any fundamentally more relevant picture than our simplistic overview will emerge. It is probably of some value to try to describe the total-spin-triplet and solitonic spin-half excitations in this description, in order to assess the theory's limitations. The triplet calculation involves locally breaking a singlet, but the solitonic calculation involves non-orthogonal states and a strong grasp of the cyclic-permutation correlation functions.

There are two quite important longer-term considerations. The states presented have correlations which extend beyond nearest neighbours. Any model with slightly longer-range interactions will therefore yield non-trivial energy from our states and can become competitive with the more widely used single-particle approaches to many-body problems. So far we have only actively considered the first hierarchy of states. Extensions to the second hierarchy ought to improve considerably the predictive power.

Appendix.

Although we will treat cyclic-exchange correlations more fully elsewhere, here we will indicate why they might be important in the current type of problem. The basic idea is that one is probing the topological domain-wall excitations. If we apply cyclic-exchange permutations of increasing range sequentially on a particular state, then we find

State	σ_N	σ_1	σ_2	σ_3	σ_4	σ_5	σ_6	σ_7
$\hat{R}_1$	σ_N*	σ_2	σ_1*	σ_3	σ_4	σ_5	σ_6	σ_7
$\hat{R}_2$	σ_N*	σ_2	σ_3	σ_1*	σ_4	σ_5	σ_6	σ_7
$\hat{R}_3$	σ_N*	σ_2	σ_3	σ_4	σ_1*	σ_5	σ_6	σ_7
$\hat{R}_4$	σ_N*	σ_2	σ_3	σ_4	σ_5	σ_1*	σ_6	σ_7
$\hat{R}_5$	σ_N*	σ_2	σ_3	σ_4	σ_5	σ_6	σ_1*	σ_7

and it is clear that we are introducing an increasing region of spins that are translated by one lattice spacing with respect to their original configuration. In creating this region we are also clearly introducing two domain walls, one at each end of the translated region. The first is found between σ_N and σ_2, and the second is found at the extraneous σ_1 (marked by $*$). As the range of the cyclic permutation is increased, so one domain wall is translated away from the other. Any divergence that shows up in the Fourier transform of these cyclic-exchange correlations can probably be interpreted as coming from low-energy domain walls in the spectrum.

On account of this interpretation, we are proposing that calculations of cyclic-exchange correlations are the correct one-dimensional probe of the 'spinon' spectrum, hence our careful analysis of these correlations.

When one considers the single-particle occupation number, $n(k) = \sum_\sigma \langle c^\dagger_{k\sigma} c_{k\sigma} \rangle$, in the context of the Hubbard model, then cyclic-exchange correlations resurface. In terms of a spin–charge separated basis, where the spins ordered along the chain are considered as

a sequential spin wavefunction, then the transfer of an electron along the chain is clearly directly related to a cyclic exchange of variable length applied to this spin wavefunction. For a single isolated hole, this cyclic exchange has a fixed length and takes us directly to a relationship between $n(k)$ and the Fourier transform of the cyclic-exchange correlations.

References

[1] Schultz H J 1991 *Int. J. Mod. Phys.* B **5** 57

[2] Majumdar C K and Ghosh D K 1969 *J. Math. Phys.* **10** 1338

[3] Hulthen L 1938 *Ark. Mat. Astr. Phys.* **26A** 1
Liang S, Doucot B and Anderson P W 1988 *Phys. Rev. Lett.* **61** 365

[4] Temperley H N V and Lieb E H 1971 *Proc. R. Soc.* A **322** 251
Bondeson S R and Soos Z G 1980 *Phys. Rev.* B **22** 1793
Long M W and Siak S 1993 *J. Phys.: Condens. Matter* **5** 5811

[5] Affleck I, Kennedy T, Lieb E H and Tasaki H 1987 *Phys. Rev. Lett.* **59** 799

[6] Bethe H A 1931 *Z. Phys.* **71** 205